

## Case study on wavelet choice based on statistical image quality measures

Igor VUJOVIĆ\*, Ivica KUZMANIĆ

Signal Processing, Analysis and Advanced Diagnostics Research and Education Laboratory,  
Department of Marine Electrical Engineering and Information Technologies, Faculty of Maritime Studies,  
University of Split, Split, Croatia

Received: 16.02.2016

Accepted/Published Online: 05.11.2016

Final Version: 30.07.2017

**Abstract:** Surveillance applications are under many negative influences, which should be suppressed, because these negative influences result in incorrectness of the motion mask. Suppression of several conflicting requirements can be optimized by a multiobjective approach. This paper proposes a multiobjective approach to selection of wavelets based on two main objectives: statistical image quality measures and execution time. Execution time is a measure of wavelets complexity. Segmentation is the final goal in order to insure precise operation of any surveillance algorithm. This paper presents a case study considering one, two, three, and four goals for wavelet selection comparison. Different wavelets are found to be an optimal choice for different weights of the objectives.

**Key words:** Wavelet transforms, video surveillance, image quality measure, multiobjective approach

### 1. Introduction

Bleeding edge video surveillance systems need to achieve several goals at the same time [1]. Therefore, a multiobjective approach can be used. The popularity of this approach is emphasized in some recent publications, such as in [2–7]. Recent studies are from the field of medical imaging, such as image registration [5] or magnetic resonance imaging [6]. Another trend is its application in oil spill detection [7]. Pareto optimum threshold can also be used for wavelet denoising purposes [8]. The proposed algorithm can be summarized as follows: select the proper thresholding function considering entropy, standard deviation (SD), peak signal to noise ratio (PSNR), and structural similarity (SSIM); perform a 2D discrete wavelet transform (DWT); optimize thresholds using adaptive multiobjective particle swarm optimization (AMOPSO); threshold the coefficients of detailed coefficients by Pareto optimal threshold; and reconstruct the image. A multiobjective approach is also used in image fusion [3,9], watermarking [10,11], and image/video coding [4,12].

DWT and image fusion based on a genetic algorithm (GA) is used in [9]. Various image fusion measures are used to evaluate the performance of the algorithm. This approach does not use multiobjective optimization, but is interesting in terms of DWT. An energy algorithm based on wavelets is also used in [3] for image fusion, but with multiobjective optimization. Watermarking is usually based on singular value decomposition (SVD) in the wavelet domain with combining the GA and multiobjective optimization [10,11].

Dual-tree DWT is used in video coding [4] and a multiobjective approach to choose an optimum subband. The optimum filter bank design based on the multiobjective approach and GA is proposed in [12]. A GA is also

\*Correspondence: ivujovic@pfst.hr

used in [13] in application to satellite images. The proposed algorithm [13] is in the class of change detection algorithms. Cost function optimization is based on the multiobjective approach. Wavelet-based transforms can also profit from the multiobjective approach. For example, curvelets are thresholded with Pareto optimized estimates in [14].

From the literature search, it can be found that there is a lack of papers dealing with multiobjective approaches with goals in the motion detection or the motion mask. However, measures in the motion mask are straightforward and easy to understand. These measures compare a ground truth and the actual results from the analyzed algorithm. We propose a new approach to wavelet selection in motion detection applications (such as traffic surveillance, security, or similar) that uses statistical quality measures comparing the motion mask and the ground truth [15]. The proposed methodology is based on the background subtraction, which is like the change detection algorithm in [13]. Moreover, a different type of measures is used in this paper.

It should be kept in mind that the algorithm used [16] is only an example, taken to illustrate the impact of the weights and the wavelet choice on the final outcome.

Motivation for this research is in the selection of the mother wavelet, which can greatly impact the final outcome even of the same algorithm. There are many types of wavelets and the need for optimum selection increases with advances in this field of signal processing. It can be observed that not every wavelet is suitable for every application or even very signal to be analyzed. Hence, results can vary significantly, because of the mother wavelet choice. That is the reason to find an optimum mother wavelet for the specific application or the specific signal.

This paper is organized as follows. The second section describes a theoretical approach to the problem solution. Firstly, definitions are given, including our modification. The second subsection describes the algorithm used. A new application of the multiobjective approach is proposed. The third section is an experimental case study for a wavelet energy algorithm with two wavelets. The multiobjective approach is used to choose the optimum wavelet pair. There are no reported studies of this kind as far as the authors are aware. The proposed multiobjective approach's influence on the wavelet choice is examined. The final section is the conclusions and discussion.

## 2. Materials and methods

Several objectives can be chosen for a final goal, depending on an application. A natural goal is to execute an algorithm as fast as possible. This is of vital importance in on-line applications. Hence, one of the possible objectives is execution time. If some wavelet combination is faster, then it is better to use it. However, the second criterion is harder to define. We want to have higher quality results. In case of, e.g. motion detection, that can be interpreted as a better segmented image (better motion mask). Statistical image quality measures offer a tool for defining "better motion mask".

### 2.1. Definitions

Firstly, we will define a multiobjective approach similar to [2] as in Definition 2.1.

**Definition 2.1** *A multiobjective approach is defined by maximizing the objective vector:*

$$\max_x g(x) = [g_1(x), g_2(x), \dots, g_M(x)]^T, \quad (1)$$

where  $x \in \chi$ , and  $\chi$  is a compact set of resources and  $M$  is a number of objectives.

Generally speaking, the problem can be defined as finding the extreme value, which could be a minimum as well as a maximum.

The most often used statistical measures are expressed as (2-5) [17-19]:

$$PCC = \frac{TP + TN}{TP + TN + FP + FN} \quad (2)$$

$$\text{precision} = \frac{TP}{TP + FP} \quad (3)$$

$$\text{recall} = \frac{TP}{TP + FN} \quad (4)$$

and

$$F = \frac{2 \cdot \text{precision} \cdot \text{recall}}{\text{precision} + \text{recall}} = \frac{2TP}{2TP + FN + FP}, \quad (5)$$

where  $TP$  denotes true positives,  $TN$  denotes true negatives,  $FP$  denotes false positives, and  $FN$  denotes false negatives.  $PCC$  is a percentage of the correct classifications, which gives information about correct detection of the moving objects. Precision measure gives a ratio between  $TP$  and the total number of pixels detected as the foreground. *Recall* measure gives information about the percentage of correctly detected foreground pixels in the total foreground.  $F$ -measure is used to describe the relationship between correctly detected foreground (motion) and a total amount of foreground pixels and pixels falsely detected as the foreground.

Goals should be defined firstly. The highest quality of the motion mask is obtained from (2) by minimizing  $FP + FN$ , which should be zero in the ideal case. Thus, in the ideal case  $PCC$  should be equal to 1. The second criterion, defined in Eq. (3), should also be equal to 1 in the ideal case. It can be obtained by minimizing  $FP$ . Ideally,  $FP$  should be 0. *Recall* should also be 1 in the ideal case. To achieve that goal  $FN$  should be minimized. Finally, from (5), the same conclusion is obtained as from (2):  $FN + FP \rightarrow 0$ .

If we summarize, actual goals that should be obtained are minimization of  $FP$ ,  $FN$ , and  $FP + FN$ . It should be noted that all three goals should be accomplished if we wish to optimize all four statistical measures expressed in Eqs. (2)–(5), because minimizing  $FN + FP$  is not the same as the minimization of  $FN$  or  $FP$  (this is illustrated in the Results section). Finally, execution time should be introduced as a goal, i.e. through frames per second ( $FPS$ ).  $FPS$  should be as high as possible and it should be maximized.

Hence, the objectives of the paper should be to maximize  $FPS$  and the motion mask quality, which can be achieved by minimization of  $FN$ ,  $FP$ , and  $FN + FP$  or maximization of Eqs. (2)–(5). The problem appears in assessing how important results are for some objectives. We can evaluate an algorithm by taking into account that all goals are equally important. In this case, we can say that  $FN$ ,  $FP$ , and  $FN + FP$  are together equally important as  $FPS$ . This should be the case when we evaluate this problem as the optimization of two objectives: image quality and time of execution. Alternatively, we can say that all four derived goals are equally important and the weights of  $FN$ ,  $FP$ ,  $FN + FP$ , and  $FPS$  are the same. Should we reach the same conclusion? This will be seen in the Results section.

Generally speaking, this line of thoughts we can define as the multiobjective approach, and it can be written as Definition 2.2.

Figure 1 shows an overall algorithm for optimal wavelet selection from a limited set of wavelet pairs, the so-called wavelet bank (WB). In general, a video sequence is analyzed by any motion detection algorithm

based on wavelets. Wavelets are taken from the WB. The obtained results are stored in the results database. If all combinations from the WB are used, the search algorithm is performed to find the best ranking wavelet combination. Hence, we can modify Definition 2.1.

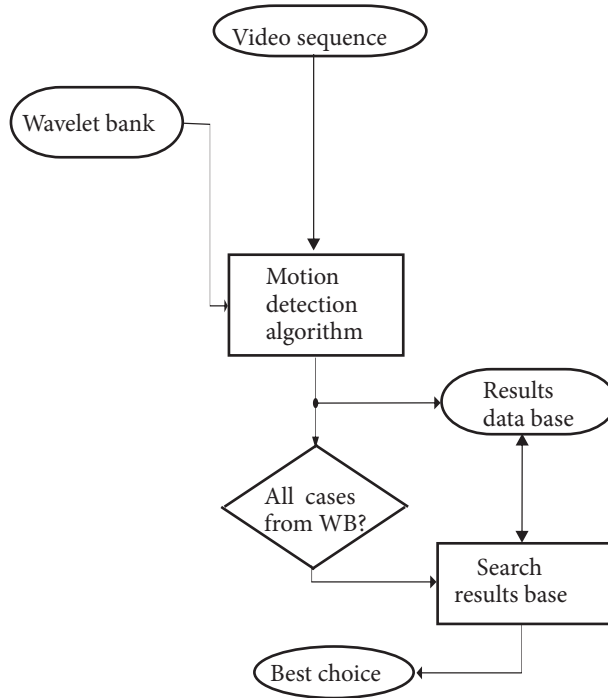


Figure 1. Algorithm for selection of the optimal wavelet.

**Definition 2.2** A video surveillance system will perform optimally if the following goals are obtained with appropriate weight (6):

$$\min g = [w_1g_1, w_2g_2, w_3g_3, w_4g_4]^T, \tag{6}$$

where  $g_1 = FN$ ,  $g_2 = FP$ ,  $g_3 = FN + FP$ ,  $g_4 = \frac{1}{FPS}$ , and  $w_1, w_2, w_3$ , and  $w_4$  are weights of the corresponding goals.

In the Results section, we will consider two cases:  $w_1 = w_2 = w_3 = w_4 = 1$  and  $w_1 = w_2 = w_3 = 1/3$  with  $w_4 = 1$ .

**Definition 2.3** A video surveillance system will perform optimally if the following goals are obtained with appropriate weight (7):

$$\max g = [w_1g_1, w_2g_2, w_3g_3, w_4g_4]^T, \tag{7}$$

where  $g_1 = TN$ ,  $g_2 = TP$ ,  $g_3 = TN + TP$ ,  $g_4 = \frac{1}{FPS}$ , and  $w_1, w_2, w_3$ , and  $w_4$  are weights of the corresponding goals.

In the Results section, we will consider two cases:  $w_1 = w_2 = w_3 = w_4 = 1$  and  $w_1 = w_2 = w_3 = 1/3$  with  $w_4 = 1$ .

**Definition 2.4** A video surveillance system will perform optimally if the following goals are obtained with appropriate weight (8):

$$\begin{cases} \min g = [w_1g_1, w_2g_2, w_3g_3, w_4g_4]^T \\ \max h = [w_5h_1, w_6h_2, w_7h_3]^T \end{cases} \quad (8)$$

where  $g_1 = FN$ ,  $g_2 = FP$ ,  $g_3 = FN + FP$ ,  $g_4 = \frac{1}{FPS}$ ,  $h_1 = FN$ ,  $h_2 = FP$ ,  $h_3 = FN + FP$ , and  $w_1, w_2, w_3, w_4, w_5, w_6$ , and  $w_7$  are weights of the corresponding goals.

In the Results section, we will consider two cases:  $w_1 = w_2 = w_3 = w_4 = w_5 = w_6 = w_7 = 1$  and  $w_1 = w_2 = w_3 = w_4 = w_5 = w_6 = 1/6$  with  $w_7 = 1$ .

The wavelets considered were orthogonal, biorthogonal, symmetrical, lazy, and Haar. We used a shorter set (20 combinations) and a larger set. The best results in the shorter set of combinations are db, sym, Haar-lazy. The shorter set is chosen heuristically, based on reports from various studies and theoretical knowledge of the best suited wavelets. Namely, a wavelet with a small number of vanishing moments has been selected in order to detect edges and a wavelet with a large number of vanishing moments has been selected in order to preserve the shape in the data. Basically, the wavelet with small number of vanishing moments is suitable for the so-called zoom effect, and the wavelet with a large number of vanishing moments is suitable for extracting shapes [20–23].

The combinations of the groups of wavelets that produced the best results in the shorter set of combinations were examined in detail. There is no need to expand all possible combinations since that would not change the research methodology.

## 2.2. Case study: wavelet energy algorithm

A motion detection algorithm based on wavelet energy is chosen as an example. The same methodology can be used for any other algorithm. The performances and characteristics of this algorithm do not fall within the scope of this paper, because it is merely provided as an example for the case study. The purpose of this section is merely to explain in general how this algorithm operates and what the important parameters are. The considered algorithm is a type of background subtraction algorithm [18]. However, instead of subtracting the current frame and the background model/frame [24], the considered algorithm subtracts the current frame’s energy and the background energy model in the wavelet domain [25–29]. The algorithm is similar to [16], but without the buffer. Therefore, most of the mathematical considerations and descriptions of details are valid here and there is no need to repeat them. The algorithm for motion detection consists of the following steps.

Step 1: Calculate the energy background model from a number of motion-free frames. Energy is calculated by two wavelets separately and then summed and normalized to obtain one matrix of energies (each matrix element corresponds to the energy of one pixel). This is performed at the second level of wavelet decomposition. The first level is performed to reduce amount of data by lazy wavelet and the lifting wavelet transform (LWT) [30]. The second level is performed by two wavelets, also by lifting. Referent single pixel energy at position (i, j) at the second level of decomposition is determined by normalizing as (9):

$$E(i, j)_{ref\_norm} = \frac{E(i, j)_{ref}}{\max(E_{ref})}, \quad (9)$$

where  $E(i, j)_{ref\_norm}$  is the normalized energy of the pixel at position (i, j) calculated in the wavelet domain,  $E(i, j)_{ref}$  not normalized energy, and  $\max(E_{ref})$  the maximal value of all pixels’ energy, which is written in

matrix  $E_{ref}$ . Matrix  $E_{ref}$  consists of pixel energies and is built as (10):

$$E_{ref} = \begin{bmatrix} E(1,1)_{ref} & E(1,2)_{ref} & \dots & E(1,m)_{ref} \\ E(2,1)_{ref} & E(2,2)_{ref} & \dots & E(2,m)_{ref} \\ \vdots & \vdots & \vdots & \vdots \\ E(n,1)_{ref} & E(n,2)_{ref} & \dots & E(n,m)_{ref} \end{bmatrix} \quad (10)$$

Step 2: Calculate the current energy matrix. This step is also performed at the second level of the wavelet decomposition.

The first level is performed by lifting of the lazy wavelet. The second level decomposition is performed by two wavelets and lifting. The result of the LWT for both wavelets is summed and normalized. The resulting energy matrix is expressed with (11):

$$E_{current\_norm} = \frac{\begin{bmatrix} E(1,1)_{current} & E(1,2)_{current} & \dots & E(1,m)_{current} \\ E(2,1)_{current} & E(2,2)_{current} & \dots & E(2,m)_{current} \\ \vdots & \vdots & \vdots & \vdots \\ E(n,1)_{current} & E(n,2)_{current} & \dots & E(n,m)_{current} \end{bmatrix}}{\max \left( \begin{bmatrix} E(1,1)_{current} & E(1,2)_{current} & \dots & E(1,m)_{current} \\ E(2,1)_{current} & E(2,2)_{current} & \dots & E(2,m)_{current} \\ \vdots & \vdots & \vdots & \vdots \\ E(n,1)_{current} & E(n,2)_{current} & \dots & E(n,m)_{current} \end{bmatrix} \right)} \quad (11)$$

Step 3: The energy matrixes obtained in steps 1 and 2 are subtracted. The result is energy difference, which is thresholded and binarized to obtain the motion mask.

The energy difference between the current energy matrix and the energy background wavelet model is calculated as (12):

$$E_{mask} = |E_{current\_norm} - E_{ref\_norm}|, \quad (12)$$

where  $E_{mask}$  denotes the energy differences matrix after subtraction. Thresholding is carried out on  $E_{mask}$  (13):

$$E_{mask\sigma 1} = \begin{cases} E_{mask} & \text{for } E_{mask} \geq \sigma_{th1} \\ 0 & \text{otherwise} \end{cases}, \quad (13)$$

where the threshold is defined with (14):

$$\sigma_{th1} = k_1 \cdot \frac{E_{current}}{\max(E_{current})} \quad (14)$$

with  $k_1 \in \mathfrak{R}^+$ . Another thresholding is performed on  $E_{mask\sigma 1}$  coefficients, as in (15):

$$E_{mask\sigma 2} = \begin{cases} E_{mask\sigma 1} & \text{for } E_{mask\sigma 1} \geq \sigma_{th2} \\ 0 & \text{otherwise} \end{cases}, \quad (15)$$

where the threshold level  $\sigma_{th2}$  is calculated as (16):

$$\sigma_{th2} = k_2 \cdot \frac{E_{mask\sigma 1}}{\max(E_{mask\sigma 1})} \quad (16)$$

with  $0 < k_2 < 1$ .

The first thresholding is the part of the algorithm used to obtain the energy difference matrix (EDM). The second thresholding is performed in order to denoise the EDM.

Step 4: The motion mask is upsampled to obtain the same number of elements as the original image frame. Upsampling is performed twice in order to obtain the same size as the original image matrix. To avoid rows and columns full of zeros, morphology is used to fill the holes. The morphology procedure consists of the morphological opening:

$$E_{m\_opening} = \sum_{k=1}^{\infty} \sum_{j=1}^{\infty} \langle E_{binarized\_mm}, MO \rangle, \quad (17)$$

where  $E_{binarized\_mm}$  represents a binarized motion mask matrix ( $E_{mask\sigma 2}$ ) and  $MO$  represents morphological opening kernel, which is used to suppress artifact pixels that could be created due to the influence of noise in the binarized motion mask matrix.

Step 5: The ground truth is compared to the obtained upsampled motion mask. Steps 2 to 5 are repeated for the entire video sequence. The algorithm is repeated for all thresholds from 1 to 8 with step 0.05, where the actual threshold is  $thr * \pi$ .

The important parameters are choice of wavelets, threshold of the energy difference, threshold for binarization, and size and shape of the structuring element in the reconstruction of the motion mask to the original size. In this research, we will analyze the influence of wavelet selection and threshold on the energy difference. Other parameters are constant.

### 3. Results

Results are obtained by usage of a publicly available dataset: video sequences called “Traffic” and “People in Shade” (IEEE Workshop on Change Detection – dataset for 2012 for “Traffic“, and 2014 for “People in Shade“; [31]). Examples of background images are provided in Figure 2. It is chosen because this sequence has enough frames to form a background model in the case study algorithm. This is only an example sequence in order to illustrate the wavelet pair selection model. Any other sequence can be used. There is no guarantee that the optimal wavelet pair will be the same if other scenes, databases, or videos are used. The point is that the optimal wavelet choice can be found for a specific scene and a letter used in that specific scene.

The set of wavelets used in the research was limited to the number of moments and family that works with a function `lwt2` in MATLAB. Combinations of wavelets are chosen heuristically to include all possible wavelet families and small and large numbers of vanishing moments. The algorithm from Section 2 (see Figure 1) is used as an example for the illustration of a multiobjective approach for wavelet choice. One can use the same methodology presented in the paper for other algorithms as well.

The Results section is organized to present cases of one, two, three, and four goals. The case of one goal considers  $FN$ , or  $FP$ , or  $FN + FP$ , or  $FPS$ . The case of two goals considers  $FPS$  and  $FN + FP$  with equal weights. The case of three goals considers  $FN$ ,  $FP$ , and  $FPS$  with equal weights. The case of four goals considers  $FN$ ,  $FP$ ,  $FN + FP$ , and  $FPS$  measures with the same weights and the case when  $FN$ ,  $FP$ , and  $FN + FP$  together have 50% of weight and  $FPS$  another 50%. The results are presented in Tables 1 and 2.

Now, we will present the obtained results. Firstly, we were interested in relations between curves  $FP$ ,  $FN$ , and  $FN + FP$  and the chosen level of threshold. This is illustrated in Figure 3, which shows that the minimums of the curves  $FP$ ,  $FN$ , and  $FN + FP$  are not obtained by the same threshold. The example shown is obtained by use of biorthogonal wavelets of order 1.3 and 1.5. It can be seen that minimum of the curve  $FP + FN$  is at  $thr = 11$ . The minimum of the curve  $FP$  can be obtained for small thresholds from 1 to 5. The minimum of



a)



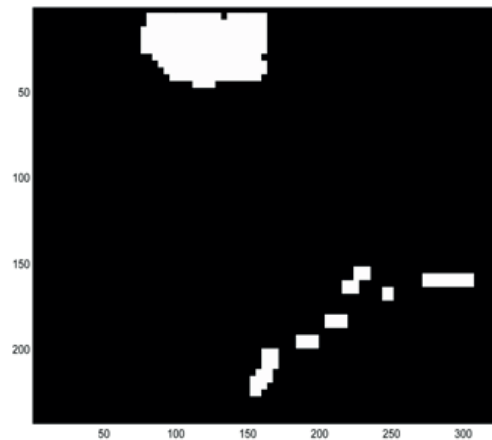
b)



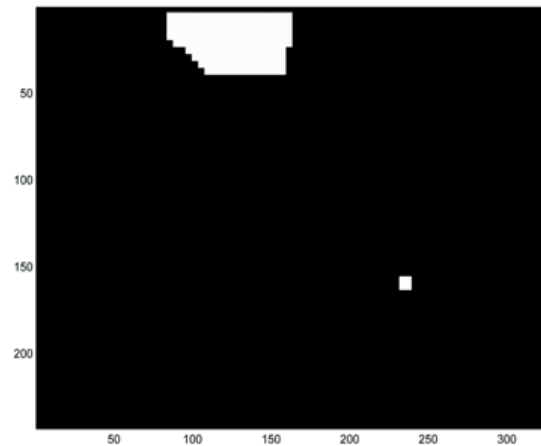
c)



d)



e)



f)

**Figure 2.** Example of: background image for “People in Shade” (a) and “Traffic” (b) sequences, c) an example image with motion, d) ground truth for (c), e) result of the algorithm for sym2–sym2 and thr = 2, f) result of the algorithm for sym2–sym2 and thr = 1.8.



the curve  $FN$  can be obtained for high thresholds. This illustrates a problem of conflicting requirements, which should be considered in the optimization problem.

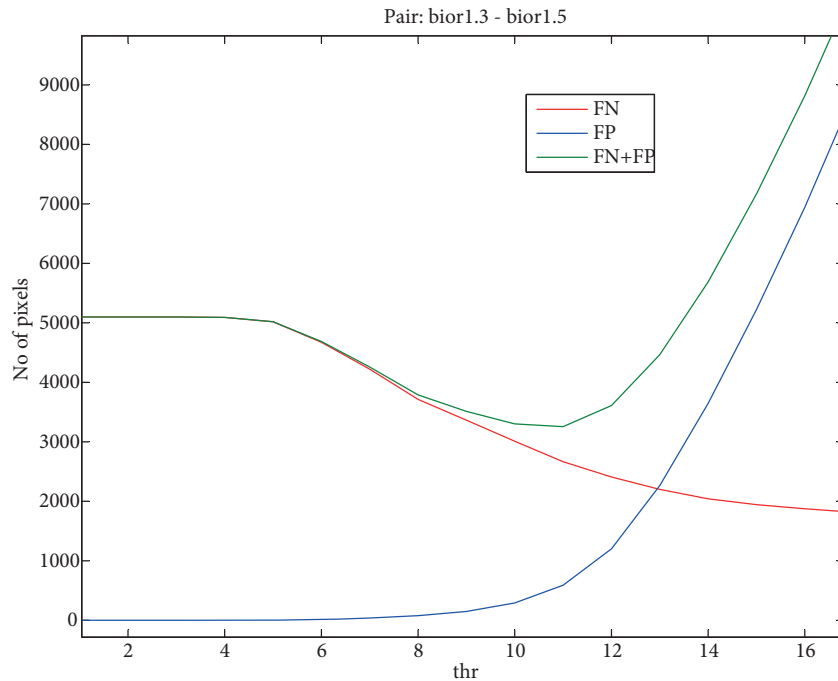


**Figure 3.** Enlarged part of curves  $FP$ ,  $FN$ , and  $FN + FP$ .

Table 1 shows experimental results for various wavelet pairs. Only the best results are presented, considering research after [16], but the point is the illustration of the method, not in wide research of all possible pairs.

One objective results: Combination of two Haar wavelets or the combination of Haar and Daubechies, db2 by MATLAB nomenclature, wavelets have the smallest  $FN$ . Table 1 also shows that two biorthogonal (bior6.8) or two Daubechies (db8) have the smallest  $FP$ . However, the pair of reverse biorthogonal spline wavelet (rbio6.8) and db6 has the smallest  $FP$  if we exclude combinations of the same wavelet. The best pair in minimization of  $FN + FP$  is bior1.3 and 1.5. The fastest execution is obtained by two lazy or two Haar wavelets. Haar-lazy combination is the fastest if we exclude the same wavelets in the pair.

Two objectives results: If we want to optimize  $FPS$  and  $FN + FP$ , then the best choice is Haar-Haar, and then Haar-lazy.

Three objective results: If we want to optimize  $FN$ ,  $FP$ , and  $FPS$ , then the best choice is bior1.3–bior5.5. This combination has almost the same results as two Haar wavelets if  $FP$ ,  $FN$ , and  $FPS$  are used as objectives (Table 2). This is correct if we want to maximize Eqs. (3) and (4).

Four objective results: The combination bior1.3 and bior5.5 is the best in the case of the same weights for  $FN + FP$ ,  $FPS$ ,  $FN$ , and  $FP$ . The results are presented in Table 2 (the first results column). This means that the lower order wavelet is used for speed and the higher order wavelet for the mask quality.

If Eq. (2) or (5) is the goal, then the best choice is two Haar wavelets (Table 2, columns 2 and 3 for 3 and 2 goals, respectively). This is also the best choice if time performance is equally important as the mask quality (the last column in Table 2). It can be seen that for such a case the second choice is the use of two second order

**Table 1.** Mean values for the entire range of thresholds and rankings by different criteria (sequence “Traffic”).

Pair	FN	FP	FPS	FN + FP	rank FN	rank FP	rank FPS	rank FN + FP	rank (FPS, FN, FP)
Haar, Haar	1169	46091	37.4138	47260	3	8	2	8	1
Haar, lazy	1171	46283	36.9598	47454	4	12	3	12	2
bior1.3, bior5.5	1165	45394	27.7939	46559	2	7	11	7	3
Haar, db2	1171	46192	33.7837	47363	5	10	7	10	4
sym2, sym2	1172	46385	35.9637	47557	6	14	6	15	5
db2, db2	1172	46385	36.5471	47557	9	16	4	14	6
bior6.8, bior6.8	2527	28530	29.3842	31057	18	3	10	3	7
db2, sym2	1172	46385	32.2021	47557	8	15	8	16	8
Haar, db8	1172	46119	25.4097	47291	7	9	16	9	9
lazy, lazy	1178	47477	41.2108	48655	11	20	1	20	10
sym8, sym8	2858	23826	27.4072	26684	19	2	12	2	11
bior2.4, coif2	5098	0	26.5591	5098	20	1	13	1	12
bior1.3, bior1.3	1186	46447	36.0005	47633	12	17	5	17	13
db2, db7	1164	46728	25.8376	47892	1	19	15	19	14
db2, db8	1176	46267	24.2406	47443	10	11	17	11	15
bior5.5, bior6.8	1756	35370	23.4867	37126	17	4	18	4	16
rbio6.8, rbio6.8	1370	42822	17.9368	44192	16	5	19	5	17
db8, db8	1187	46344	26.2897	47531	13	13	14	13	18
rbio6.8, db6	1246	44928	15.2795	46174	15	6	20	6	19
bior1.3, bior1.5	1188	46546	31.3225	47734	14	18	9	18	20

Symlets. The third option is the combination of lazy and Haar. This is the first option if we exclude the same wavelets from the considerations.

Similar observations can be made in Tables 3–5. Table 3 shows results for the “People in Shade” sequence and Definition 2.2. Haar–lazy combination is the best if the *FPS* has the same weight as the total of other parameters. Table 4 provides results for the same sequence and Definition 2.3. In this case, the best combination is db2–db2. Table 5 shows results for Definition 2.4 for the same sequence. In this case, for 50% *FPS* and 50% other parameters, the winner is lazy–lazy, db2–db2 is the runner-up, and Haar–lazy is in third place.

The spread in the execution speed is shown as percentage of the mean *FPS*. The formula for calculations is shown in the last column of Table 6. The smallest spread of *FPS* is obtained by two bior6.8 wavelets. The largest is obtained by two db2 wavelets. This can lead to conclusions about the stability of the algorithm execution in MATLAB.

#### 4. Discussion and conclusions

The scope of the paper is not the wavelet energy algorithm but the multiobjective approach to wavelet selection. The algorithm used was taken as an example to experimentally validate the theoretical conclusions. The same methodology, but possibly with other consequences, can be used for other measures, statistical and nonstatistical, and other algorithms.

From the results, one can conclude differently if mean results for all thresholds (for statistical and *FPS* measures) are used and if only the optimal threshold is used. However, optimal is hard to define, as illustrated in Figure 1.

We can see that the best choice of wavelets (in the used set) is, for equal weights of *FN*, *FP*, *FN +*

**Table 2.** Experimental results for considered rankings by Definition 2.2. (“Traffic” sequence).

Wavelet pair	rank FN, FP, FN + FP, FPS (equal weights)	rank FN, FP, FPS (equal weights)	rank FN + FP, FPS (equal weights)	Weighted rank: 50% mask 50% time
Haar, Haar	2	1	1	1
sym2, sym2	4	1	3	2
Haar, lazy	3	4	2	3
lazy, lazy	10	6	7	4
bior1.3, bior5.5	1	1	4	5
Haar, db2	5	6	4	6
db2, db2	8	8	6	6
bior1.3, bior 1.3	6	5	9	8
db2, sym2	7	9	7	9
bior1.3, bior1.5	12	11	11	10
bior6.8, bior6.8	16	10	15	11
Haar, db8	11	13	12	12
rbio6.8, db6	9	12	10	13
sym8, sym8	14	17	16	13
db2, db8	13	14	13	15
db8, db8	17	18	14	15
rbio6.8, rbio6.8	15	15	16	17
db2, db7	18	16	16	17
bior5.5, bior6.8	19	19	19	19

**Table 3.** Experimental results for considered rankings by Definition 2.2 (“People in Shade” sequence).

Wavelet pair	rank FN, FP, FN + FP, FPS (equal weights)	rank FN, FP, FPS (equal weights)	rank FN + FP, FPS (equal weights)	Weighted rank: 50% mask (FN and FP together), 50% time (FPS)
Haar, Haar	18	14	13	7
sym2, sym2	7	10	17	16
db8, db8	1	2	11	11
sym8, sym8	2	8	1	8
rbio6.8, rbio6.8	3	9	2	10
db2, sym2	4	4	4	6
bior2.4, coif2	5	15	3	14
bior1.3, bior1.5	6	5	8	4
Haar, db2	8	3	7	2
bior6.8, bior6.8	9	11	5	13
Haar, lazy	10	1	6	1
bior5.5, bior6.8	11	12	14	15
db2,db2	12	6	9	5
Haar, db8	13	17	15	17
lazy, lazy	14	7	10	3
bior1.3, bior1.3	15	13	12	9
db2, db7	16	18	16	18
db2, db8	17	19	19	19
bior1.3, bior5.5	19	16	18	12
rbio6.8, db6	20	20	20	20

**Table 4.** Experimental results for considered rankings by Definition 2.3 (“People in Shade” sequence).

Wavelet pair	rank TN, TP, TN + TP, FPS (equal weights)	rank TN, TP, FPS (equal weights)	rank TN + TP, FPS (equal weights)	Weighted rank: 50% mask (TN and TP together), 50% time (FPS)
db2,db2	1	1	2	1
db8, db8	2	4	10	11
lazy, lazy	3	2	3	2
sym8, sym8	4	9	1	7
bior6.8, bior6.8	5	11	5	9
db2, db7	6	6	11	10
bior2.4, coif2	7	14	5	14
db2, db8	8	8	15	13
rbio6.8, rbio6.8	9	13	6	12
Haar, Haar	10	3	7	3
db2, sym2	11	12	8	8
Haar, lazy	12	5	9	4
bior1.3, bior1.5	13	10	13	6
bior5.5, bior6.8	14	16	14	17
Haar, db2	15	7	12	5
sym2, sym2	16	19	19	19
Haar, db8	17	18	17	18
bior1.3, bior5.5	18	15	18	16
bior1.3, bior1.3	19	17	16	15
rbio6.8, db6	20	20	20	20

**Table 5.** Joint positive and negative logic criteria – optimum solution for “People in Shade” sequence based on equal weights (Definition 2.4).

Wavelet pairs	rank FPS	rank TN	rank TP	rank TN + TP	rank FN	rank FP	rank FN + FP	Total rank (equal all weights)	Total rank (50% mask, 50% FPS)
db8, db8	18	1	5	2	2	5	5	1	12
sym8, sym8	9	18	2	3	19	2	2	2	4
bior2.4, coif2	13	19	1	1	20	1	1	3	11
bior6.8, bior6.8	11	16	3	4	17	4	4	4	9
rbio6.8, rbio6.8	12	17	4	5	16	3	3	5	10
db2, db2	4	4	9	9	14	11	14	6	2
bior5.5, bior6.8	17	15	6	6	10	6	7	7	16
db2, sym2	8	13	11	10	8	10	8	8	7
sym2, sym2	20	12	10	11	1	9	6	9	19
db2, db7	14	6	7	7	18	7	11	10	14
bior1.3, bior1.5	7	10	13	14	6	13	10	11	7
db2, db8	16	5	8	8	15	8	13	11	17
Haar, db2	5	9	15	16	5	15	12	13	5
lazy, lazy	1	3	16	12	12	16	18	14	1
Haar, lazy	2	7	18	17	3	18	15	15	3
Haar, db8	15	14	12	13	9	12	9	16	18
Haar, Haar	3	2	19	15	11	19	20	17	6
bior1.3, bior5.5	10	8	20	19	4	20	19	18	15
bior1.3, bior1.3	6	20	14	20	13	14	17	19	13
rbio6.8, db6	19	11	17	18	7	17	16	20	20

**Table 6.** Spread of FPS (minimum and maximum, “Traffic” sequence).

Wavelet pair	Min	Max	Mean	FPS range = (max-min)/mean
bior1.3, bior1.3	35.1968	36.92	36.0005	4.7866%
bior1.3, bior1.5	30.4529	32.0497	31.3225	5.0979%
bior1.3, bior5.5	27.3462	28.2302	27.7939	3.1806%
bior2.4, coif2	26.0121	27.1271	26.5591	4.1982%
bior5.5, bior6.8	23.0341	23.824	23.4867	3.3632%
bior6.8, bior6.8	28.938	29.8565	29.3842	3.1258%
db2, db2	33.4996	37.3999	36.5471	10.6719%
db2, db7	25.205	26.293	25.8376	4.2109%
db2, db8	23.8043	24.643	24.2406	3.4599%
db2, sym2	31.233	32.9174	32.2021	5.2307%
db8, db8	25.6579	26.7946	26.2897	4.3237%
Haar, db2	33.1337	34.4113	33.7837	3.7817%
Haar, db8	24.9977	26.0586	25.4097	4.1752%
Haar, lazy	36.2952	37.677	36.9598	3.7386%
lazy, lazy	40.0183	43.0493	41.2108	7.3548%
rbio6.8, db6	14.4168	15.8678	15.2795	9.4970%
rbio6.8, rbio6.8	17.6243	18.401	17.9368	4.3302%
sym2, sym2	35.3116	37.2641	35.9637	5.4291%
sym8, sym8	26.8301	27.854	27.4072	3.7359%

*FP*, and *FPS*, the combination of bior1.3 and bior5.5. The best choice of wavelets (in the tested set) is a pair consisting of two Haar wavelet for *FN*, *FP*, *FN + FP*, and *FPS* criteria with equal weights for *FPS* and total of statistical measures (1/3 all criteria). When considering the case of *FP*, *FN*, and *FPS* criteria with the same weights, the best choice of wavelets is two Haar wavelets or the combination of bior1.3 and bior5.5. Finally, we can conclude that the choice of wavelets depends on the criteria chosen and the weights of specific criteria.

The disadvantage of the presented research is in the limitation of wavelets to be selected. However, the methodology is the same for a larger set of wavelet pairs. We randomly choose combinations of wavelets, which operate with *lwt2* function in MATLAB (there are restrictions). Hence, it is possible that a larger set of mother wavelets could lead to different conclusions about the best optimal choice of wavelets. An interesting further direction of the research could be standardization of the mother wavelet set used for the analysis. It should reduce the number of trials per video sequence.

The initial hypothesis of this study was that optimum wavelet pairs should be a combination of the same wavelet families with different moments—a small number of moments for execution speed and large number of moments for mask precision (not statistical measure precision, but joint *FN*, *FP*, and/or *TP/TN* criteria). However, the results in Tables 2–5 show that the best results for the same number of moments are obtained if all weights are equal, for example, in the “People in Shade” sequence, the db8 and db8 combination for Definition 2.4, which means that we do not need a combination of wavelets at all. The best combination of different wavelets by the same definition is bior2.4 and coif2. If we need to weight *FPS* by 50% and other parameters with 50%, then the most suitable combination is lazy and lazy, and Haar and lazy are the best different wavelet combination. Hence, it is obvious that chosen wavelets greatly depend on weights (importance of specific parameters).

Since when the results in Tables 2 and 3 (Definition 2.2 for the “Traffic” and “People in Shade” sequences) for e.g. 50% *FPS* and 50% other parameters weight are compared, the best combination is Haar–lazy for the “People in Shade” and Haar–Haar for “Traffic”, the results might be concluded to vary from sequence to sequence, but since Haar–lazy is in the top 3 in both cases, it could be a relatively safe combination for this weight.

Finally, there is the question of why are lazy, Haar, or Daubechies more powerful wavelets. It is because of weights, which was important for the research. When weight of *FPS* is 50% and other parameters in total 50%, then the most important parameter is execution speed. Hence, wavelets with small computational complexity are more powerful, such as lazy, Haar, or similar. If we choose different weights, it is possible to obtain better results with other wavelets.

### References

- [1] Panda DK. Motion detection, object classification and tracking for visual surveillance application. MSc, National Institute of Technology Rourkela, Odisha, India, 2012.
- [2] Björnson E, Jorswieck E, Debbah M, Ottersten B. Multiobjective signal processing optimization – the way to balance conflicting metrics in 5G systems. *IEEE Signal Proc Mag* 2014; 31: 14-23.
- [3] Xie Q, Long Q, Mita S, Guo C, Jiang A. Image fusion based on multi-objective optimization. *Int J Wavelets Multi* 2014; 12: 1450017.
- [4] Thamarai M, Shanmugalakshmi R. Multi objective particle swarm optimization in video coding. *Int J Soft Computing Eng* 2013; 2: 419-423.
- [5] Pirpinia K, Alderliesten T, Sonke JJ, van Herk M, Bosman PAN. Diversifying multi-objective gradient techniques and their role in hybrid multi-objective evolutionary algorithms for deformable medical image registration. In: *GECCO'15 Annual Conference on Genetic and Evolutionary Computation*; 11–15 July 2015; Madrid, Spain. New York, USA: ACM. pp. 1255-1262.
- [6] Limam OM. MRI segmentation based on multiobjective fuzzy clustering. *J Biomed Eng Med Imaging* 2016; 3: 7-13.
- [7] Marghany M. Multi-objective entropy evolutionary algorithm for marine oil spill detection using cosmo-skymed satellite data. *Ocean Sci Discuss* 2015; 12: 1263-1289.
- [8] Niu YF, Shen LC. Wavelet denoising using the Pareto optimal threshold. *IJCSNS Int J Comput Sci Net Sec* 2007; 7: 30-34.
- [9] Dammavalam SR, Maddala S, Mhm KP. Quality assessment of pixel-level image fusion using fuzzy logic. *Int J Soft Comput* 2012; 3: 11-23.
- [10] Loukhaoukha K. Image watermarking algorithm based on multiobjective ant colony optimization and singular value decomposition in wavelet domain. *J Opt* 2013; 2013: 921270.
- [11] Loukhaoukha K, Chouinard JY, Taieb MH. Multi-objective genetic algorithm optimization for image watermarking based on singular value decomposition and lifting wavelet transform. In: *Proceedings 4th International Conference on Image and Signal Processing*; 30 June –2 July 2010; Trois-Rivières, QC, Canada. New York, NY, USA: Springer. pp. 394-403.
- [12] Boukhobza A, Taleb Ahmed A, Taleb N, Bounoua A. Optimization design of orthogonal filter banks for image coding via multi-objective genetic algorithm. Seminar, Université Hassiba Benbouali de Chlef, Chlef, Algeria, 2010.
- [13] Çelik T, Yetgin Z. Change detection without difference image computation based on multiobjective cost function optimization. *Turk J Elec Eng & Comp Sci* 2011; 19: 941-956.
- [14] Niu YF, Shen LC. A novel approach to image denoising using the Pareto optimal curvelet thresholds. In: *Proceedings of the International Conference on Wavelet Analysis and Pattern Recognition*; 2–4 November 2007; Beijing, China. New York, NY, USA: IEEE. pp. 630-635.

- [15] Avciabas I, Sankur B, Sayood K. Statistical evaluation of image quality measures. *J Electron Imaging* 2002; 11: 206-223.
- [16] Vujović I, Šoda J, Kuzamanić I (2013). Stabilising illumination variations in motion detection for surveillance applications. *IET Image Process* 7: 671-678.
- [17] Rosin P, Ioannidis E. Evaluation of global image thresholding for change detection. *Pattern Recogn Lett* 2003; 24: 2345-2356.
- [18] Elhabian SY, Sayed KME, Ahmed SH. Moving object detection in spatial domain using background removal techniques - state-of-art. *Recent Patents Comput Sci* 2008; 1: 32-54.
- [19] Cheung SCS, Kamath C. Robust techniques for background subtraction in urban traffic video. In: *Proceedings SPIE Visual Communications and Image Processing*; 18 January 2004; San Jose, USA. Bellinghama, Washington, USA: SPIE. pp. 881-892.
- [20] Daubechies I. *Ten Lectures on Wavelets*. Philadelphia, PA, USA: SIAM, 1992.
- [21] Mallat S. *A Wavelet Tour of Signal Processing*. New York, NY, USA: Academic Press, 2009.
- [22] Vetterli M, Kovačević J. *Wavelets and Subband Coding*. New York, NY, USA: Prentice-Hall, 1995.
- [23] Roșca D. *Wavelets on two-dimensional manifolds*. Habilitation thesis, Technical University of Cluj-Napoca, Cluj-Napoca, Romania, 2012.
- [24] Lazarevic N. *Background modelling and performance metrics for visual surveillance*. PhD, Kingston University, Kingston upon Thames, UK, 2011.
- [25] Vujović I, Šoda J, Beroš SM. Time-frequency methods in maritime surveillance systems. *NMore* 2012; 59: 254-265.
- [26] Herley C, Kovačević J, Ramchandran K, Vetterli M. Tilings of the time-frequency plane: construction of arbitrary orthogonal bases and fast tiling algorithms. *IEEE T Signal Proces* 1993; 41: 3341-3359.
- [27] Kingsbury N. The dual-tree complex wavelet transform: a new efficient tool for image restoration and enhancement. In: *Proceedings European Signal Processing Conference*, 8–11 September 1998; Rhodes, Greece; London: EURASIP. pp. 319-322.
- [28] Selesnick IW, Baraniuk RG, Kingsbury NG. The dual-tree complex wavelet transform. *IEEE Signal Proc Mag* 2005; 22: 123-151.
- [29] Rioul O, Vetterli M. Wavelets and signal processing. *IEEE Signal Proc Mag* 1991; 8: 14-38.
- [30] Sweldens W. The lifting scheme: a construction of second generation wavelets. *SIAM J Math Anal* 1998; 29: 511-546.
- [31] Goyette N, Jodoin PM, Porikli F, Konrad J, Ishwar P. *changedetection.net: A new change detection benchmark dataset*. In: *Proceedings IEEE Workshop on Change Detection*; 16–21 June 2012; Providence, RI, USA. New York, NY, USA: IEEE. pp. 1-9.